

Neutron diffraction study of magnetically ordered $\text{Tm}_2\text{Fe}_3\text{Si}_5$

A. R. Moodenbaugh and D. E. Cox

Physics Department, Brookhaven National Laboratory, Upton, New York 11973

C. B. Vining*

*Ames Laboratory, U.S. Department of Energy, Ames, Iowa 50011
and Department of Physics, Iowa State University, Ames, Iowa 50011*

(Received 23 April 1985)

$\text{Tm}_2\text{Fe}_3\text{Si}_5$ has been studied at low temperatures by neutron powder diffraction techniques. At $T=1.5$ K the diffraction pattern is characteristic of a tetragonal crystal structure, space group $P4/mnc$ (D_{4h}^6 ; with $a=10.332$ Å and $c=5.388$ Å), similar to that of the prototype compound $\text{Sc}_2\text{Fe}_3\text{Si}_5$. Below $T=1.2$ K magnetic scattering peaks develop, which can be indexed with the parameters of the chemical cell. A noncollinear antiferromagnetic structure is proposed which features ordering of Tm moments in the $\langle 110 \rangle$ set of directions. The magnetic moment of Tm is $6.5\mu_B$ at the lowest temperature attained, 0.35 K.

INTRODUCTION

$\text{Tm}_2\text{Fe}_3\text{Si}_5$ has attracted much interest due to the fact that both superconductivity and magnetism appear in this compound.^{1,2} An antiferromagnetic transition occurs near a Néel temperature $T_N=1.15$ K. Mutual inductance measurements have shown, in addition to the magnetic transition, a partial (i.e., a few percent) superconducting transition below 2.0 K, and a full superconducting transition above about 3 kbar.^{1,2}

$\text{Tm}_2\text{Fe}_3\text{Si}_5$ is a member of the tetragonal $M_2\text{Fe}_3\text{Si}_5$ family, space group $P4/mnc$ (D_{4h}^6 ; prototype $\text{Sc}_2\text{Fe}_3\text{Si}_5$).³⁻⁵ Superconductivity is observed in these materials when the rare-earth atom M is nonmagnetic, in spite of the high concentration of iron.⁶ The appearance of superconductivity is even more unusual in $\text{Tm}_2\text{Fe}_3\text{Si}_5$ since Tm is itself a magnetic atom.^{1,2}

Previous work on $\text{Tm}_2\text{Fe}_3\text{Si}_5$ includes specific-heat measurements, which show, in contrast to the multiple specific-heat anomalies observed in $\text{Tb}_2\text{Fe}_3\text{Si}_5$ and $\text{Er}_2\text{Fe}_3\text{Si}_5$, only a single anomaly, near $T=1.1$ K.⁷ Mössbauer studies on other members of this family of compounds are consistent with the iron being nonmagnetic.⁸⁻¹¹

The present neutron diffraction study of $\text{Tm}_2\text{Fe}_3\text{Si}_5$ is an extension of previous work on $\text{Tb}_2\text{Fe}_3\text{Si}_5$ (Ref. 12) and $\text{Er}_2\text{Fe}_3\text{Si}_5$ (Ref. 13). In each of the earlier studies, two magnetic structures were observed. Just below T_N an incommensurate structure appeared. Then, at lower temperatures corresponding to those at which additional specific-heat anomalies occur, commensurate magnetic phases appeared. However, in the case of $\text{Tm}_2\text{Fe}_3\text{Si}_5$ only a single transition, to a commensurate structure, near $T=1.15$ K is observed.

SAMPLE PREPARATION
AND EXPERIMENTAL METHODS

A 5-g sample of $\text{Tm}_2\text{Fe}_3\text{Si}_5$ was prepared. Fe and Si were first melted in a copper hearth arc furnace under a

Ti-gettered Ar atmosphere, following which the Tm was melted into the alloy in the same furnace. The ingot was heat treated in a metal element vacuum furnace for 4 days at 1200°C. In this step about 3% of the original mass was lost from evaporation and/or by spalling.

An x-ray diffraction scan of a powder sample of the final product was performed on a General Electric XRD-5 diffractometer equipped with diffracted beam monochromator, using Cu $K\alpha$ radiation. In addition to the expected peaks for $\text{Tm}_2\text{Fe}_3\text{Si}_5$, several weak impurity peaks of intensity up to 3% of the most intense peak were seen. Room-temperature lattice parameters determined from the x-ray diffraction scan were $a=10.37$ Å and $c=5.405$ Å.

Neutron diffraction scans were performed at the Brookhaven National Laboratory High Flux Beam Reactor with a neutron wavelength of 2.38 Å. A pyrolytic graphite monochromator and analyzer were set for the (002) reflection, higher-order contamination being suppressed with a graphite filter. Collimation was set at 20', 40', 40', and 40', respectively, for in-pile, monochromator-sample, sample-analyzer, and analyzer-detector locations. The powder sample was contained in an Al sample holder inside a pumped ^3He Dewar. Neutron scans over the range $2\theta=10^\circ$ to 70° were performed at two temperatures, $T=1.5$ K, above T_N , and at 0.32 K, the lowest temperature studied. At intermediate temperatures, various scans of individual peaks were made. Superconducting properties were determined by low-temperature mutual inductance measurements performed on a solid portion of the sample.

RESULTS

Portions of the full neutron diffraction scans are shown in Fig. 1. At 1.5 K [Fig. 1(a)], most of the peaks can be indexed on the basis of the chemical cell. Impurity peaks are also present in the pattern, the most obvious being at $2\theta=44.2^\circ$. Several additional unidentified peaks, overlap-

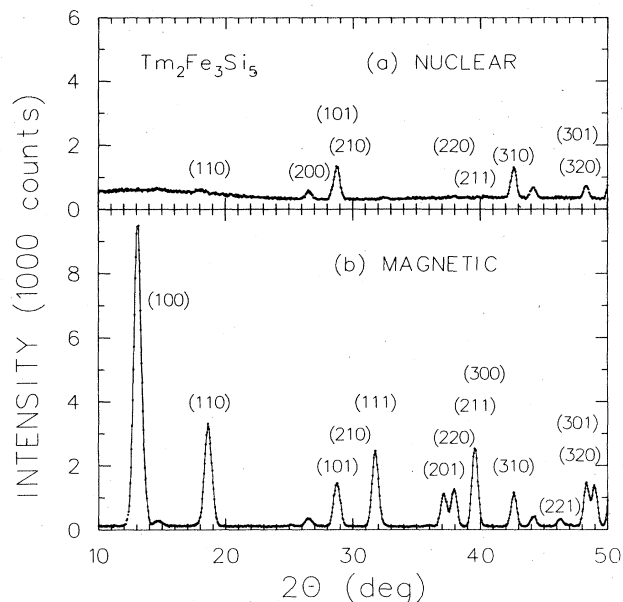


FIG. 1. Portions of neutron diffraction scans of $\text{Tm}_2\text{Fe}_3\text{Si}_5$ at (a) 1.5 K and at (b) 0.35 K. The neutron wavelength was 2.38 Å. Nuclear scattering peaks are indexed in (a); magnetic peaks only are indexed in (b).

ping the nuclear peaks, are also apparent. The presence of these impurity peaks precluded analysis by the Rietveld profile technique utilized in earlier studies.^{12,13} However, individual and overlapping peaks were fit with Gaussian peak shape(s) by a least-squares procedure which varied peak positions, amplitudes, and full widths at half maximum. Results of these fits provide accurate peak positions and intensities for characterizing the chemical structure.

The model chosen for the chemical structure was assumed to have $P4/mnc$ symmetry with tetragonal cell parameters $a = 10.332$ Å and $c = 5.388$ Å. Positional parameters, which are assumed to be the same as those determined in the Rietveld refinement for the structure of $\text{Er}_2\text{Fe}_3\text{Si}_5$,¹³ are as follows:

$$\text{Tm: } x=0.072, y=0.236;$$

$$\text{Fe}_1: x=0.377, y=0.358;$$

$$\text{Si}_1: x=0.175;$$

$$\text{Si}_2: z=0.246;$$

$$\text{Si}_3: x=0.185, y=0.476.$$

Neutron scattering lengths were taken from the compilation of Koester,¹⁴ and temperature factors were set equal to zero in the calculations. Table I lists the peak positions

TABLE I. Calculated (I_{calc}) and observed (I_{obs}) integrated intensities for nuclear ($T=1.5$ K) and combined nuclear and magnetic scattering ($T=0.35$ K) below $2\theta=60^\circ$. Calculated 2θ 's and hkl 's are listed. Observed 2θ 's agree with calculated values to within $\pm 0.02^\circ$. Impurity peaks are denoted by an asterisk. The large discrepancy between observed and calculated intensities for (400) at 54.89 is also attributed to an overlapping impurity peak. (Dashes appear at positions forbidden in the nuclear pattern.)

hkl	$2\theta_c$	Nuclear		Nuclear and magnetic		
		I_{calc}	I_{obs}	I_{calc}	I_{obs}	
100	13.23	—	—	5869	6547(110)	
110	18.76	4	0	2063	2082(30)	
200	26.65	144	128(15)	144	156(10)	
	28.28*		≈ 40			
101	28.86	531	543(20)	838	801(18)	
210	29.86	≈ 0	≈ 0	44	≈ 0	
111	31.87	—	—	1096	1350(37)	
	32.36*		≈ 20			
201	37.24	—	—	718	552(20)	
220	38.04	13	20(5)	595	616(20)	
211	39.68	≈ 0	2(5)	1621	1343(30)	
300	40.45	—	—	≈ 0	18(18)	
310	42.74	484	466(20)	506	520(20)	
	44.10*		≈ 180			
221	46.38	—	—	41	125(9)	
301	48.44	163	188(10)	698	666(21)	
320	49.10	15	2(4)	560	607(20)	
311	50.44	677	707(26)	1120	1220(30)	
	51.68*		≈ 50			
002	52.45	275	291(12)	275	250(12)	
102	54.35	—	—	830	742(24)	
400	54.89*	2	50	2	*	
321	56.11	121	559(10)	382	1128(35)	
112	56.20	462				1083
410	56.73	451				

and intensities, calculated using the above model, which can be compared with observed intensities obtained from the least-squares fits, from which it is seen that agreement is generally good.

Below $T_N=1.15$ K additional peaks developed, as shown by the diffraction pattern at $T=0.35$ K [Fig. 1(b)]. These peaks may be attributed to antiferromagnetic order, as indicated by the previously reported susceptibility¹ and specific-heat⁷ data. With the exception of a small peak at $2\theta=14.6^\circ$, the magnetic cell can be indexed with the lattice parameters of the chemical cell, but exhibits a different set of systematic absences as shown by the magnetic Bragg indices in Fig. 1(b).

The pattern observed at 0.35 K was decomposed into integrated intensities using the same least-squares routine described above. The magnetic intensities can be well accounted for by a noncollinear model of antiferromagnetic order of the Tm moments as illustrated in Fig. 2. Tm positions in four adjacent cells are shown projected on the (001) plane, with the Tm moments arranged along the $\langle 110 \rangle$ set of directions as represented by the arrows.

The calculated nuclear peak intensities and positions were assumed to be the same as at 1.5 K, and the magnetic intensities at 0.35 K were calculated with a Tm moment $\mu=6.5\mu_B$, ordered as in Fig. 2, utilizing calculated spherical form factors for Tm.¹⁵ Good agreement is seen between the calculated and observed intensities (see Table I), the estimate of the uncertainty in the moment being $\pm 0.3\mu_B$.

The relative intensity of the (100) magnetic peak was determined as a function of temperature. From these measurements, the variation of the Tm moment as a function of temperature may be determined normalized to the value of $6.5\mu_B$ found at 0.35 K. The monotonic variation is consistent with the observation of only a single magnetic phase.

Mutual inductance measurements were carried out on a portion of the $\text{Tm}_2\text{Fe}_3\text{Si}_5$ sample (see Fig. 4). The behavior observed is typical of that previously observed at

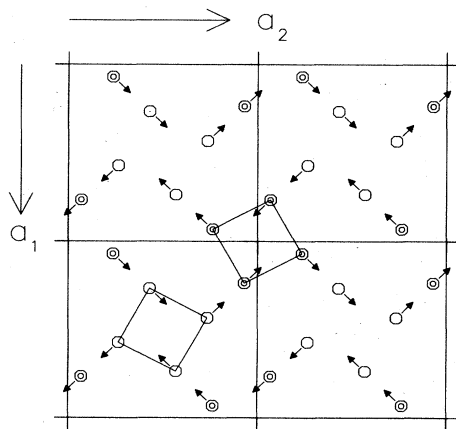


FIG. 2. Illustration of Tm atomic positions in four adjacent chemical cells, projected on the (001) plane. Cell edges are shown by straight solid intersecting lines. Tm atoms at $z=0$ are represented by shaded symbols; atoms at $z=c/2$ by open symbols. Arrows represent moment directions. Line connecting Tm atoms describe near-neighbor (001) squares.

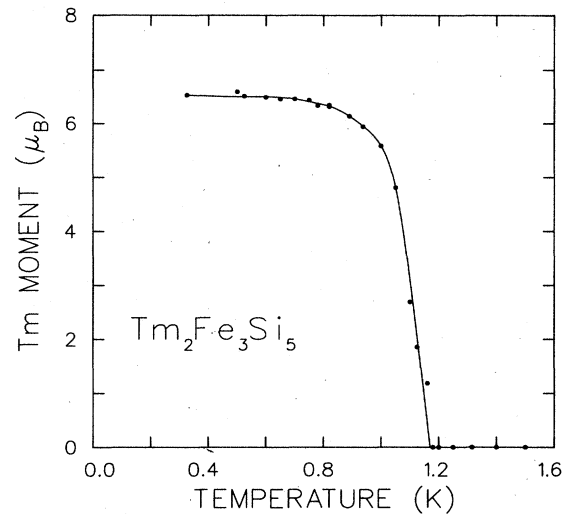


FIG. 3. Magnetic moment of Tm as a function of temperature. See the text for details.

atmospheric pressure,¹ and may be interpreted as follows. Above $T=2$ K the susceptibility increases as the temperature is reduced, as is characteristic of antiferromagnets above T_N . Below 2 K there is a downturn in the susceptibility which we attribute to a partial (i.e., a few percent) superconducting transition. This slight degree of superconductivity may be strain-induced, since it is known that $\text{Tm}_2\text{Fe}_3\text{Si}_5$ becomes fully superconducting near a pressure of 3 kbar.² For example, a similar partial (nonbulk) strain-induced superconducting transition is often observed in uranium, which also becomes a bulk superconductor at a pressure of a few kbar.^{16,17} Below 1.2 K, an upturn in the susceptibility of $\text{Tm}_2\text{Fe}_3\text{Si}_5$ signifies the end of the superconducting transition, and the increase in the Pauli paramagnetism above T_N resumes. Near 1.05 K the susceptibility reaches a maximum, and the sharp dropoff below T_N is again the expected behavior for an antiferromagnet. Neutron diffraction scans were performed in

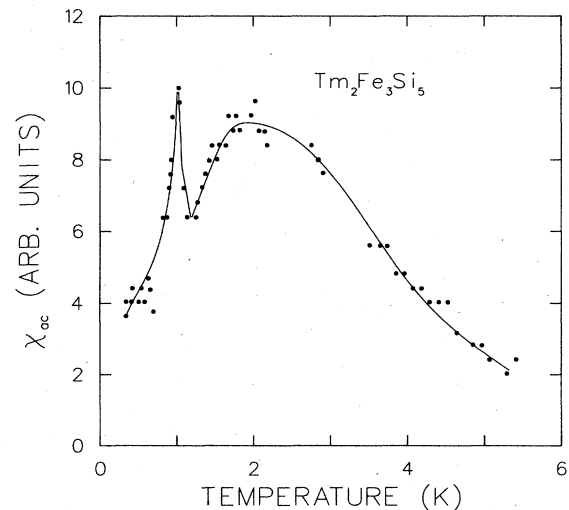


FIG. 4. Mutual inductance (susceptibility) measurements, χ_{ac} on $\text{Tm}_2\text{Fe}_3\text{Si}_5$. A value of -150 for χ_{ac} corresponds to an approximately full superconducting transition.

the region between 2.0 K and 1.2 K in a search for magnetic diffraction peaks, since the susceptibility results could possibly be interpreted as magnetic ordering near 2 K. No evidence of such peaks was observed, however. Thus the neutron diffraction results are consistent with the interpretation of the susceptibility results given above.

The above model does not account for the small peak at $2\theta=14.6^\circ$ noted above. Within experimental error this peak has the same T_N and temperature dependence as the (100) peak, and may therefore reflect a slight long-range modulation of the structure shown in Fig. 2.

SUMMARY

This neutron diffraction study has determined the nature of the antiferromagnetic ordering in $\text{Tm}_2\text{Fe}_3\text{Si}_5$ below the Néel temperature of 1.15 K. As in earlier investigations of $M_2\text{Fe}_3\text{Si}_5$, the rare earth, Tm, is the sole contributor to magnetic order.⁸⁻¹² Unlike the cases of the Tb and Er compounds studied previously by neutron diffraction,^{12,13} only one magnetic phase is observed (down to

$T=0.35$ K). The magnetic moments order within the (001) plane, and are directed in the $\langle 110 \rangle$ set of directions. In this respect, the magnetic structure has much in common with the commensurate model proposed for $\text{Er}_2\text{Fe}_3\text{Si}_5$.¹³ The main difference is that moments on diagonally opposite corners of the basal plane squares (Fig. 2) are antiparallel in $\text{Tm}_2\text{Fe}_3\text{Si}_5$, but parallel in the Er compound.

ACKNOWLEDGMENTS

The work performed at Brookhaven National Laboratory was supported by the Division of Materials Sciences, U.S. Department of Energy, under Contract No. DE-AC02-76CH00016. Ames Laboratory is operated for U.S. Department of Energy by Iowa State University under Contract No. W-7405-Eng-83, and research performed there is supported by the Director for Energy Research, Office of Basic Sciences, under Contract No. WPAS-KC-02-02-02.

*Present address: General Electric Company, P.O. Box 8555, Philadelphia, PA 19101.

¹C. U. Segre and H. F. Braun, *Phys. Lett.* **85A**, 372 (1981).

²C. B. Vining and R. N. Shelton *Solid State Commun.* **54**, 53 (1985).

³O. I. Bodak, V. K. Pecharskii, and E. I. Gladyshevskii, *Izv. Akad. Nauk SSSR, Neorg. Mater.* **14**, 250 (1978) [*Inorg. Mater. (USSR)* **14**, 188 (1978)].

⁴O. I. Bodak, B. Ya. Kotur, V. I. Yarovets, and E. I. Gladyshevskii, *Kristallografiya* **22**, 385 (1977) [*Sov. Phys.—Crystallogr.* **22**, 217 (1977)].

⁵H. F. Braun, in *Ternary Superconductors*, edited by G. K. Shenoy, B. D. Dunlap, and F. Fradin (Elsevier—North-Holland, New York, 1981), p. 225.

⁶H. F. Braun, *Phys. Lett.* **75A**, 386 (1980).

⁷C. B. Vining and R. N. Shelton, *Phys. Rev. B* **28**, 2732 (1983).

⁸J. D. Cashion, G. K. Shenoy, D. Niarchos, P. J. Viccaro, and C. M. Falco, *Phys. Lett.* **79A**, 454 (1980).

⁹H. F. Braun, C. U. Segre, F. Acker, M. Rosenberg, S. Dey, and

P. Deppe, *J. Magn. Mater.* **25**, 117 (1981).

¹⁰J. D. Cashion, G. K. Shenoy, D. Niarchos, P. J. Viccaro, A. T. Aldred, and C. M. Falco, *J. Appl. Phys.* **52**, 2180 (1981).

¹¹D. R. Noakes, G. K. Shenoy, D. Niarchos, A. M. Umarji, and A. T. Aldred, *Phys. Rev. B* **27**, 4317 (1983).

¹²A. R. Moodenbaugh, D. E. Cox, and H. F. Braun, *Phys. Rev. B* **25**, 4702 (1982).

¹³A. R. Moodenbaugh, D. E. Cox, C. B. Vining, and C. U. Segre, *Phys. Rev. B* **29**, 271 (1984).

¹⁴L. Koester, in *Neutron Physics*, Vol. 80 of *Springer Tracts in Modern Physics*, edited by G. Hoehner (Springer, Berlin, 1977), Chap. 8.

¹⁵M. Blume, A. J. Freeman, and R. E. Watson, *J. Chem. Phys.* **37**, 1245 (1962).

¹⁶J. C. Ho, N. E. Phillips, and T. F. Smith, *Phys. Rev. Lett.* **17**, 694 (1966).

¹⁷J. E. Gordon, H. Montgomery, R. J. Noer, and G. R. Pickett, *Phys. Rev.* **152**, 432 (1966).